

Description and simulation of physics of Resistive Plate Chambers

V. Français

*Université Clermont Auvergne, Université Blaise Pascal, Université Blaise Pascal, CNRS/IN2P3, LPC,
4 Av. Blaise Pascal, TSA/CS 60026, F-63178 Aubière, France*

Abstract

Monte-Carlo simulation of physical processes is an important tool for detector development as it allows to predict signal pulse amplitude and timing, time resolution, efficiency . . . Yet despite the fact they are very common, full simulations for RPC-like detector are not widespread and often incomplete. They are often based on mathematical distributions that are not suited for this particular modelisation and over-simplify or neglect some important physical processes.

We describe the main physical processes occurring inside a RPC when a charged particle goes through (ionisation, electron drift and multiplication, signal induction ...) through the Riegler-Lippmann-Veenhof model together with a still-in-development simulation. This is a full, fast and multi-threaded Monte-Carlo modelisation of the main physical processes using existing and well tested libraries and framework (such as the Garfield++ framework and the GNU Scientific Library). It is developed in the hope to be a basic ground for future RPC simulation developments.

Keywords: Resistive-plate chambers, Detector modelling and simulations II, Gaseous detectors

1. Introduction

Resistive Plate Chambers (RPC) are gaseous particle detectors widely used in many High Energy Physics experiments as they are affordable and yet efficient and reliable (compared to scintillator-based detectors), both as timing or tracking charged-particle detector.

A RPC is basically made of gaseous mixture contained between two plates of resistive materials (typically Bakelite or glass) where a high-voltage is applied between them, typically from 1 to 10 kV.

A charged particle going through the detector will ionise the gas, freeing one or more electrons. Those freed electrons, under the influence of the electric field, will drift toward the anode and multiply by interactions with gas molecules and finally produce an electronic avalanche. Typically RPCs are operated with a mixture of three gases: a ionising gas ($\sim 95\%$), an UV quencher gas ($\sim 4\%$) which absorbs photons in order to avoid secondary avalanches, an electron quencher gas ($\sim 1\%$) which absorbs a fraction of the electrons to contain the avalanche.

We present results with the mixture used by CALICE SDHCAL [9]: TFE $C_2H_2F_4$ (93%), CO_2 (5%) and SF_6 (2%). We use a common single-gap RPC geometry: the gas-gap is 1.2 mm wide, the anode and cathode are respectively 0.7 and 1.1 mm thick with a dielectric constant of $\epsilon_r = 7$.

2. Primary ionisation

When a charged particle traverses the detector it ionises the gas mixture in several zones, by emission of photo-electrons and auto-ionisation (Auger) electrons. Those zones then contain 1 or more freed electrons which are called electron clusters. The energy deposit is then characterized by the number of clusters produced by unit of length as well as the probability distribution for the number of electrons per cluster. On average a minimum ionising muon produces about 75 clusters by cm as shown by figure 1(a). Most of the time a cluster contains 1 electron then the probability drops rapidly with the number of electrons and for instance, for 4 GeV/c muons, is below 1% for more than 5 electrons, as shown on figure 1(b). Those values are computed with the HEED simulation program [4] and are in good accordance with experimental results [4, 1].

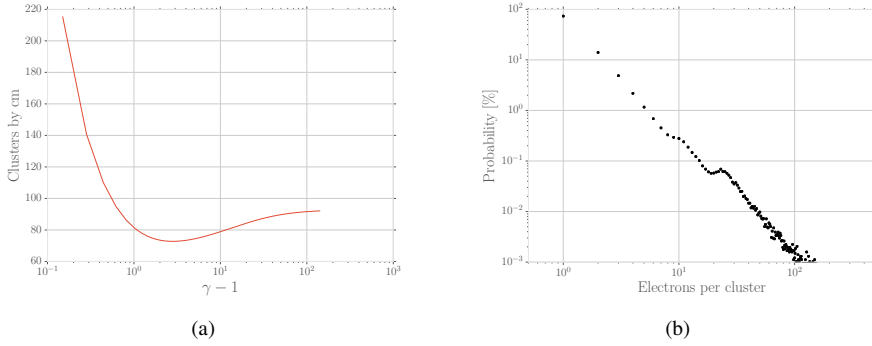


Figure 1: (a) Number of clusters produced by unit of length in function of the particle energy, here a muon. (b) Probability distribution for the number of electrons produced per cluster for 4 GeV/c muons.

3. The Riegler-Lippmann-Veenhof model for electronic avalanche

The electrons freed during ionisation will then drift towards the anode under the influence of the electric field, and start an electronic avalanche by multiplying while interacting with gas molecules. In this section we briefly detail the Riegler-Lippmann-Veenhof model for electronic avalanche [1] which is a continuation of the Legler model for avalanche in electro-negative gas [10].

3.1. Electron multiplication

The avalanche development is characterised by the Townsend coefficient α and the attachment coefficient η . If an avalanche contains n electrons at the position x , the probability it contains $n + 1$ at $x + dx$ is given by $n\alpha dx$. In the same way, the probability that one electron gets attached in an avalanche containing n electrons is given by $n\eta dx$. Then the average numbers of electrons \bar{n} and positive ions \bar{p} are modelised following [1]

$$\frac{d\bar{n}}{dx} = (\alpha - \eta)\bar{n}, \quad \frac{d\bar{p}}{dx} = \alpha\bar{n}. \quad (1)$$

With the initial condition $\bar{n}(0) = 1$ and $\bar{p}(0) = 0$ this yields

$$\bar{n}(x) = e^{(\alpha-\eta)x}, \quad (2)$$

$$\bar{p}(x) = \frac{\alpha}{\alpha - \eta} \left(e^{(\alpha-\eta)x} - 1 \right). \quad (3)$$

In order to observe an electronic avalanche the exponential in eq. 2 has to be positive. Figure 2(a)

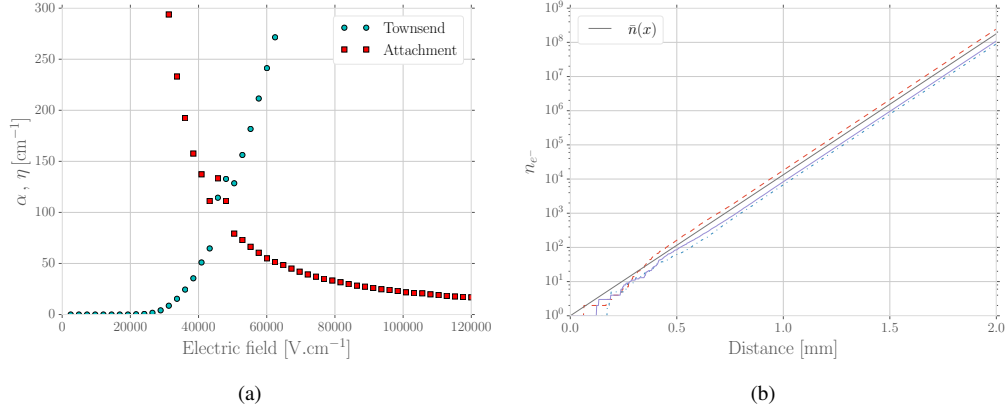


Figure 2: (a)Townsend and attachment coefficients α and η as a function of the electric field, for the gaseous mixture of $\text{C}_2\text{H}_2\text{F}_4/\text{CO}_2/\text{SF}_6$ (93%/5%/2%). Values are computed with Magboltz 9.01 [7]. (b) Simulation of three distinct avalanches started by one electron at $x = 0$. The analytic formulation for the average number of electrons (eq. 2) is also plotted on the figure.

shows both coefficients in function of the intensity of the electric field. In this case, the electric field needs to be greater than 49 kV/cm for an avalanche to develop.

The evolution of the number of electrons in an avalanche is modelised following [1]

$$n = \begin{cases} 0, & s < k \frac{\bar{n}(x)-1}{\bar{n}(x)-k} \\ 1 + \ln \left(\frac{(\bar{n}(x)-k)(1-s)}{\bar{n}(x)(1-k)} \right) \frac{1}{\ln \left(1 - \frac{1-k}{\bar{n}(x)-k} \right)}, & s > k \frac{\bar{n}(x)-1}{\bar{n}(x)-k} \end{cases} \quad (4)$$

where s is a random number $\in [0, 1)$ and $k = \eta/\alpha$. Eq. 4 is valid only for $\alpha, \eta > 0$, details for the other cases are in [1]. In order to calculate the induced signal we can't use the probability distribution to approximate the final avalanche charge, instead we have to simulate the actual avalanche development. The gas gap is divided in N steps of Δx . In the case we have n_0 electron at the position x_0 , we'll find n_1 electrons at the position $x = x_0 + \Delta x$ according to eq. 4. Meaning that we loop over the n_0 electrons, draw a number from eq. 4 and sum them. In the same way the n_1 electrons will multiply and we'll have n_2 electrons at $x = x_0 + 2\Delta x$. This procedure is iterated until all the electrons have reached the anode.

The figure 2(b) shows the simulation of three avalanches started by one electron at the cathode. The first interactions at beginning of the avalanches has an important influence for their development, and they quickly behave like an positive exponential just like the average number of electrons $\bar{n}(x)$ given by eq. 2.

It is also important to note that an avalanche is not only driven by $(\alpha - \eta)$, but also by α and η themselves as pointed out in [1].

3.2. Diffusion

When no electric field is present, an electron cloud in a gas is subject to the classic thermal diffusion. But when an electric field is applied the thermal diffusion motion is superposed by a drift motion. At the microscopic scale an electron drifting the distance δz gains the energy $e_0 |\vec{E}| \delta z$ between two collisions, where $|\vec{E}|$ is the intensity of the field and e_0 the unit charge. Some of this energy will be lost during the next encounter with a gas molecule (non-ionising elastic collision). Then the electron is again accelerated by the electron field and lost some when colliding, and so on. At a macroscopic scale one sees the electron moving with a constant drift velocity which depends on the gas and the electric field applied [6].

Because of this constant drift motion superposed to the thermal diffusion motion, the diffusion becomes anisotropic. We can separate it in two distinct terms, a longitudinal one and a transverse one [6]

$$\varphi_L(z, l) = \frac{1}{\sqrt{2\pi}\sigma_L} \exp\left(-\frac{(z-z_0)^2}{2\sigma_L^2}\right) \quad (5)$$

$$\varphi_T(z, l) = \frac{1}{\sigma_T^2} \exp\left(-\frac{(r-r_0)^2}{2\sigma_T^2}\right) \quad (6)$$

We used cylindrical coordinate and rotational symmetry (a ϕ -integration was carried out leading to an additional factor of 2π). The width of the Gaussian depends on the longitudinal and transverse diffusion coefficients $D_{L,T}$ [$\sqrt{\text{cm}}$] and the drifted distance l : $\sigma_{L,T} = D_{L,T} \sqrt{l}$. Figure 3(a) shows the dependence of the diffusion coefficient on the electric field.

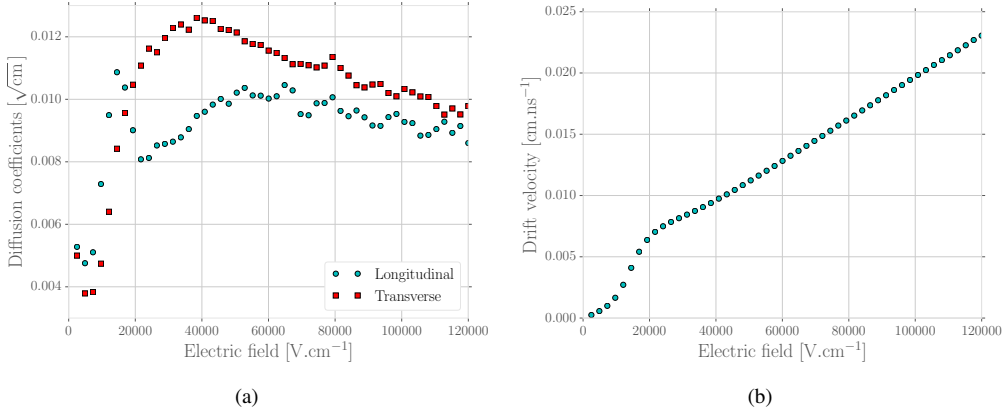


Figure 3: (a) Longitudinal and transverse diffusion coefficient as a function of the electric field. (b) Electron drift velocity as a function of the field intensity. Both are computed with MAGBOLTZ 9.01 [7]

In the simulation the longitudinal diffusion is fully modelised: the electrons are redistributed at each simulation step where the new z -coordinate is computed by drawing a random number from eq. 5, where $\sigma_L = D_L \sqrt{\Delta z}$ and Δz is the detector step which is the distance drifted by the electrons between two simulation steps. However the transverse diffusion is only approximate as the avalanche is modelised in 1-dimension. We suppose the electrons are contained in a disc perpendicular to the z -axis with a radial charge distribution following eq. 6 with $\sigma_t = D_T \sqrt{l}$ with l the distance drifted by the electrons from their position of generation.

3.3. Space Charge Effect

This section briefly details the Space Charge Effect in an RPC. The general solution is detailed in [3] and a description of this effect in RPC can be found in [2, 6].

When the number of charges in the avalanche becomes high enough they influence the electric field, and so influence the values of the Townsend and attachment coefficient α and η . This is the Space Charge Effect. We need to compute the contribution to the electric field of all the charges present in the avalanche. The analytic formula for the potential $\Phi(r, \phi, z, r', \phi', z')$ of a point charge in an infinite plane condenser of three layers is detailed in [2, 3]. (r, ϕ, z) is the point of observation and (r', ϕ', z') is the position of the charge. Since the simulation is in 1-dimension it is sufficient to compute $\Phi(r = 0, \phi = 0, z, r', \phi' = 0, z') = \Phi(z, r', z')$. As we only approximate the transverse diffusion where we consider a unit charge at position z' is contained in a disk perpendicular to the z -axis, the electric field of this disk is given by [6, 2]

$$\bar{E}(z, l, z') = - \int_0^{\infty} \varphi_T(r', l) \frac{\partial \Phi(z, r', z')}{\partial z} r' dr \quad (7)$$

where φ_T is the radial charge distribution of the disk (eq. 6). The total field from the space charges is then computed by summing over the disk at each detector bin:

$$E_{SC}(z) = \sum_{n=0}^N q_n \bar{E}(z_n, l_n, z'_n) \quad (8)$$

where q_n is total charge in bin n .

3.4. Induced current

In order to compute the induced current we make use of the Ramo's theorem generalised to resistive materials [8, 5]

$$i(t) = e_0 N(t) v_e \frac{\epsilon_r}{(d_{r_1} + d_{r_2}) + \epsilon_r d_g} \quad (9)$$

where $N(t)$ is the number of electrons in the detector at time t , ϵ_r is the relative dielectric constant of the resistive layers, d_g and d_{r_i} are respectively the width of the gas gap and of the resistive layers. v_e is the electron drift velocity, it depends on the gas mixture as well as the electric field. It is shown on figure 3(b) as a function of the field intensity.

4. Results

The charges induced over time is shown on figure 4(a). One can note a clear saturation effect at about time step 350, due to the Space Charge Effect as the number of charges became high enough to lower the applied field and thus the multiplication gain. Figure 4(b) is a simulated efficiency curve along with the time-resolution. The efficiency is the ratio of the number of avalanches that has crossed the detection threshold (set to 100 fC) to the total number of avalanches simulated. The time-resolution is taken as the standard-deviation from the threshold-crossing time distribution, i.e. the time when the induced charge has crossed the detection threshold. For the RPC configuration we considered in the simulation, at its operation point of 6.9 kV, the experimental efficiency is about 96% with a typical time resolution around 500 ps [9] which are in good accordance with figure 4(b).

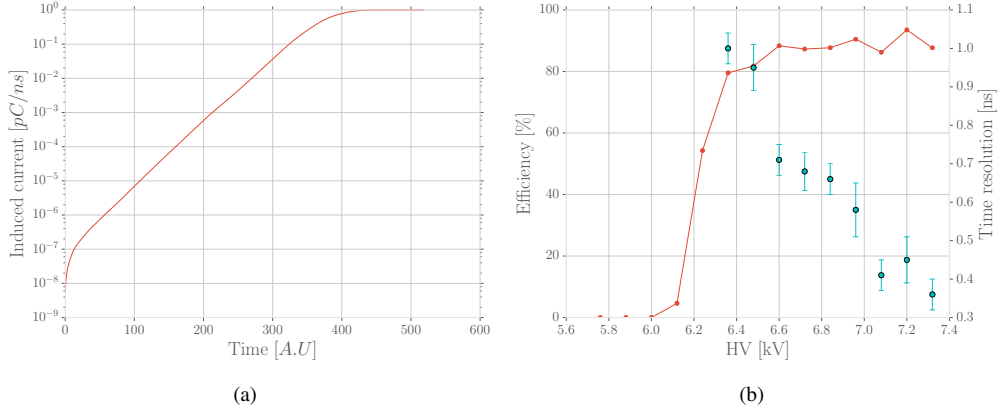


Figure 4: (a) Induced charges during an avalanche as function of time (arbitrary unit) for 5 GeV/c muons. (b) Simulated efficiency and time-resolution for 5 GeV/c muons.

5. Conclusion

We have briefly detailed the main physical processes having an important impact for the electronic avalanches occurring in a RPC, through the Riegler-Lippmann-Veenhof model. The results produced by the simulation show good behavior but could be compared to experimental data from test beam. In this so-called 1.5D model, the transverse diffusion is only approximated while a full 2-dimensional simulation would be, rationally, more accurate but also much slower. This model calls for a lot of matrix algebra, thus taking advantage of the computing power of GPUs for this matter could provide a non-negligible speed-up.

References

- [1] W. Riegler, C. Lippmann, R. Veenhof, *Detector physics and simulation of resistive plate chambers*, *Nucl. Instr. and Meth. A* **500** (2003) 144.
- [2] W. Riegler, C. Lippmann, R. Veenhof, *Space charge effects in Resistive Plate Chambers*, *Nucl. Instr. and Meth. A* **517** (2004) 54.
- [3] Th. Heubrandtner, B. Schnizer, C. Lippmann, W. Riegler, *Static electric fields in an infinite plane condenser with one or three homogeneous layers*, CERN-OPEN 2001-074 (2001).
- [4] I. Smirnov, *Modeling of ionization produced by fast charged particles in gases*, *Nucl. Instr. and Meth. A* **554** (2005) 474.
- [5] W. Riegler, *Induced signals in resistive plate chambers*, *Nucl. Instr. and Meth. A* **491** (2002) 258.
- [6] C. Lippmann, *Detector Physics of Resistive Plate Chambers*, PhD Thesis (2003).
- [7] S. Biagi, *Monte Carlo simulation of electron drift and diffusion in counting gases under the influence of electric and magnetic fields*, *Nucl. Instr. Meth. A* **421** (1999) 234.
- [8] S. Ramo, *Currents induced by electron motion*, *Proc. IRE* **27** (1939) 584.
- [9] The CALICE collaboration, *First results of the CALICE SDHCAL technological prototype*, *JINST* **11** (2016) P04001.
- [10] W. Legler, *Die Statistik der Elektronenlawinen in elektronegativen Gasen bei hohen Feldstärken und bei großer Gasverstärkung*, *Zeitschrift für Naturforschung A* **16** (1961) 253.